

Application of the relativistic local-density approximation to photoionization of the outer shells of neon, argon, krypton, and xenon

F. A. Parpia, W. R. Johnson, and V. Radojević*

Department of Physics, University of Notre Dame, Notre Dame, Indiana 46556

(Received 30 January 1984)

Parameters describing the low-energy photoionization of the outer shells of the rare gases Ne, Ar, Kr, and Xe have been calculated using a relativistic generalization of the time-dependent local-density approximation. The resulting photoionization cross sections, angular-distribution asymmetry parameters, and spin polarization parameters are presented here. The results are found to be in good agreement with those from the relativistic random-phase approximation (RRPA), even though the present theory is simpler, formally and computationally, than the latter. These results, and those of the RRPA, are generally in good agreement with experiment, illustrating the utility of the present approach to photoionization, especially for heavy atoms in which both relativistic and correlation effects are important.

I. INTRODUCTION

The time-dependent local-density approximation (TDLDA) developed by Zangwill and Soven¹ is a simple yet powerful theory for the calculation of photoionization cross sections. For atoms with high nuclear charge it has been well established that spin-orbit interaction must be taken into account.² The spin-orbit interaction and other relativistic effects are included in the relativistic time-dependent local-density approximation (RTDLDA),³⁻⁵ which is a relativistic generalization of the TDLDA.

The RTDLDA describes the linear response of an atomic ground state to a time-dependent external field; it is closely related to another linear-response theory, the relativistic random-phase approximation (RRPA),^{6,7} which is the relativistic version of the random-phase approximation [RPA—often called the RPA with exchange (RPAE), as well as the time-dependent Hartree-Fock approximation].⁸⁻¹¹ In the case of the RTDLDA the ground state is described by the relativistic local-density approximation (RLDA),^{12,13} while for the RRPA, the ground state of the

system is given by the Dirac-Fock (DF) approximation. These two theories differ since the expressions for the ground-state energy as a functional of the ground-state orbitals are different. The DF ground-state energy functional contains the usual sum of one-electron, direct, and exchange terms, whereas the RLDA functional contains an estimate of the correlation correction to the energy as well. In the RLDA expression both the exchange and correlation terms are approximated as those of a homogeneous electron gas of the appropriate density. Since exchange and correlations are incorporated by a local potential, the RTDLDA is simpler than the RRPA. Details of the RTDLDA and RRPA formalisms have been given in the literature.³⁻⁷ An application of the RTDLDA to the photoionization of Hg, and a description of the formalism in the context of photoionization, have also appeared.^{3,4}

In this paper we present the results of our calculations of photoionization parameters in the RTDLDA for the rare-gas atoms Ne, Ar, Kr, and Xe, and compare them with the same parameters calculated in the RRPA^{7,14,15} and in certain cases with those calculated in the RPA by

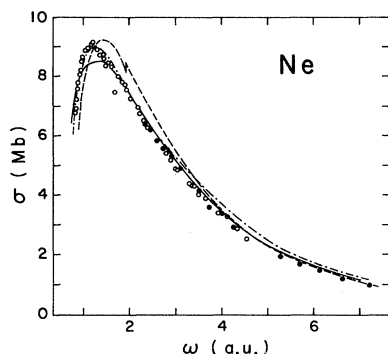


FIG. 1. Total photoionization cross section for Ne as a function of photon energy ω . Experiment: \cdots , Marr and West (Ref. 20); \circ , Samson (Ref. 18); \bullet , Watson (Ref. 19). Theory: — , RTDLDA, this work; --- , RRPA, Johnson and Cheng (Ref. 7).

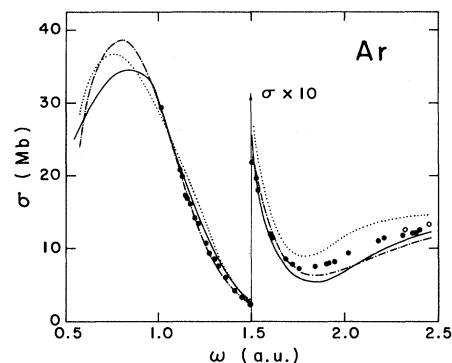


FIG. 2. Total photoionization cross section for Ar as a function of photon energy ω . Experiment: \cdots , Marr and West (Ref. 20); \bullet , Samson (Ref. 18); \circ , Watson (Ref. 19). Theory: — , RTDLDA, this work; --- , RRPA, Johnson and Cheng (Ref. 7).

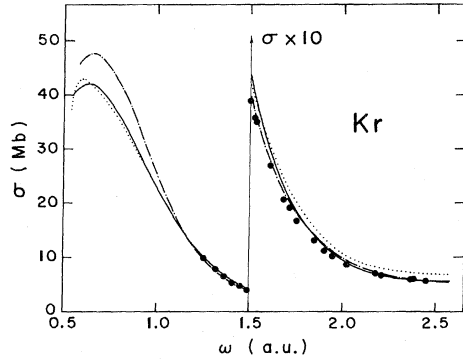


FIG. 3. Total photoionization cross section for Kr as a function of photon energy ω . Experiment: \cdots , Marr and West (Ref. 20); \bullet , Samson (Ref. 18). Theory: --- , RTDLDA, this work; - - - , RRPA, Johnson and Cheng (Ref. 7).

Amusia and Cherepkov¹⁰ and by Cherepkov,¹⁶ as well as with the corresponding experimental data. Although all of the parameters have been calculated both in the RTDLDA and RRPA, we have restricted our attention here to those quantities for which extensive experimental data are available. Each of the sections II–VII of this paper is dedicated to the discussion of a single photoionization parameter for all four rare gases.

All calculations have been carried out in the dipole approximation. The photoionization differential cross section for a subshell with quantum numbers n, l, j is given by¹⁷

$$\frac{d\sigma_{nlj}}{d\Omega} = \frac{\sigma_{nlj}}{4\pi} \left[1 - \frac{1}{2} \beta_{nlj} P_2(\cos\theta) \right].$$

Here θ is the angle between the direction of the incident photon and the outgoing photoelectron. The quantities σ_{nlj} and β_{nlj} are, respectively, the partial cross section and the photoelectron angular-distribution asymmetry parameter for a given subshell. In the present analysis only correlations between the outermost subshells are considered. For Ne and Ar, seven dipole excitation channels are included,

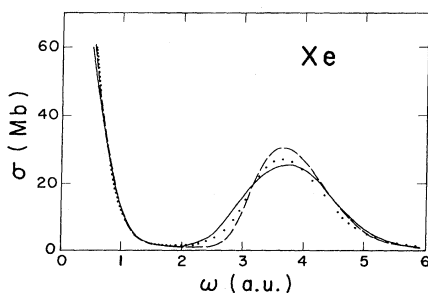


FIG. 4. Total photoionization cross section for Xe as a function of photon energy ω . Experiment: \cdots , West and Morton (Ref. 21). Theory: --- , RTDLDA, this work; - - - , RRPA, Johnson and Cheng (Ref. 7).

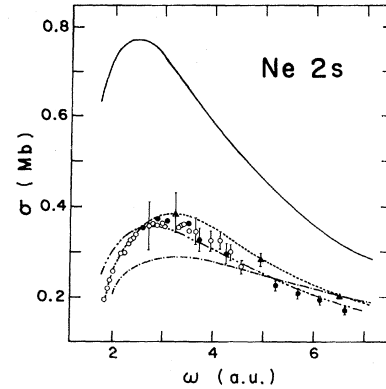


FIG. 5. Partial photoionization cross section of the $2s$ shell of Ne as a function of the photon energy ω . Experiment: \blacklozenge , Marr and West (Ref. 20); \blacklozenge , Samson (Ref. 18); \blacklozenge , Watson (Ref. 19). Theory: --- , RTDLDA, this work; - - - , RRPA, Johnson and Cheng (Ref. 7); - \cdot - \cdot - , RPAE, Amusia and Cherepkov (Ref. 10).

$$ns_{1/2} \rightarrow p_{3/2}, p_{1/2},$$

$$np_{1/2} \rightarrow d_{3/2}, s_{1/2},$$

$$np_{3/2} \rightarrow d_{5/2}, d_{3/2}, s_{1/2},$$

while in the cases of Kr and Xe, six more channels,

$$(n-1)d_{3/2} \rightarrow f_{5/2}, p_{3/2}, p_{1/2},$$

$$(n-1)d_{5/2} \rightarrow f_{7/2}, f_{5/2}, p_{3/2},$$

are included.

The results obtained are not independent of the form of the exchange-correlation potential used. In Sec. VIII a comparison is made of three different exchange-correlation potentials, and the particular choice made for

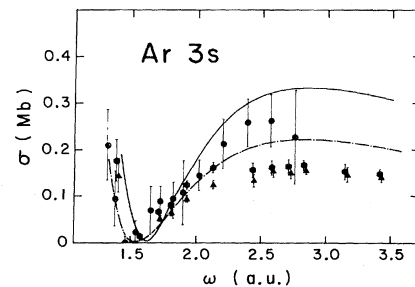


FIG. 6. Partial photoionization cross section of the $3s$ shell of Ar as a function of the photon energy ω . Experiment: \blacklozenge , Tan and Brion (Ref. 24); \blacklozenge and \blacklozenge , Adam *et al.* (Ref. 25), scaled by total cross section from Marr and West (Ref. 20), and Samson (Ref. 18), respectively. Theory: --- , RTDLDA, this work; - - - , RRPA, Johnson and Cheng (Ref. 7).

the applications considered here, the Perdew-Zunger potential, is justified.

II. TOTAL CROSS SECTIONS

The total RTDLDA cross sections for Ne, Ar, Kr, and Xe are presented in Figs. 1–4, respectively, where the RTDLDA results are compared with the theoretical RRPDA results^{7,15} and with experimental data.^{18–21}

The RTDLDA curve for the total cross section of Ne, shown as the solid line in Fig. 1, has some structure in the region of its maximum. This structure is due to the onset of the contribution of the $2s$ shell. In the case of the RTDLDA this onset is not as pronounced²² as in the RRPDA case, shown as the dashed curve, where a sharp rise appears at the $2s$ threshold. For both the RTDLDA and the RRPDA, the threshold of a particular subshell is the negative of the eigenvalue of the corresponding one-electron orbital equation.^{4,6} The RLDA eigenvalue is larger (less negative) than the DF eigenvalue. This results in an overall shift to lower energy of the RTDLDA curve with respect to that of the RRPDA. We note that the RTDLDA provides a very good description of the total experimental cross section of Ne^{18–20} except in the region near the maximum.

In the case of Ar, shown in Fig. 2, both the RRPDA and RTDLDA are in good agreement with the existing measurements^{18–20} away from the threshold. This behavior is repeated for Kr as shown in Fig. 3, although the discrepancies between the RTDLDA and the experimental measurements^{18,20} diminish appreciably for Kr as compared with Ne and Ar.

For Xe, as seen in Fig. 4, the agreement of both the RTDLDA and the RRPDA with recent experimental data²¹ is, contrary to the previous cases, better near the threshold than away from it. In the region of energies farther away from the threshold (starting at about 5 a.u.) both the RTDLDA and the RRPDA results agree well with experimental data. For energies above the energy of the cross-section minimum (about 2 a.u.), the contribution to the total cross section comes mainly from the $4d$ shell. The broad maximum of the Xe $4d$ cross section between about 2.5 and 5 a.u. is sometimes interpreted as a collective resonance.²³ It is to be noted that both the RTDLDA and the RRPDA reproduce the general shape of the total experi-

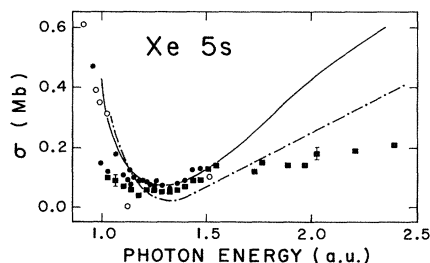


FIG. 7. Partial photoionization cross section of the $5s$ shell of Xe as a function of the photon energy ω . Experiment: \circ , Samson and Gardner (Ref. 26); \bullet , Gusstafson (Ref. 27); \blacksquare , Fahlman *et al.* (Ref. 28). Theory: —, RTDLDA, this work; ---, RRPDA, Johnson and Cheng (Ref. 7).

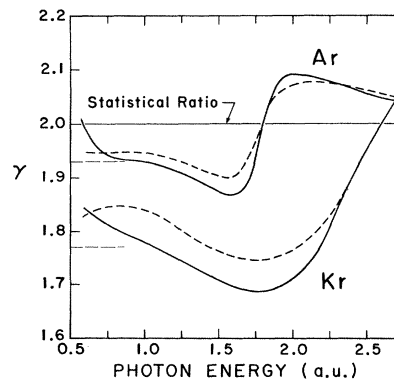


FIG. 8. Branching ratio of the np shells of Ar and Kr as a function of photon energy ω . Experiment: —, Samson *et al.* (Ref. 30). Theory: —, RTDLDA, this work; ---, RRPDA, Johnson and Cheng (Ref. 7).

mental cross-section curve, although discrepancies remain between the theories and experiment.

III. PARTIAL CROSS SECTIONS OF THE ns SHELLS

In Figs. 5–7 we present the RTDLDA cross-section contributions of the ns shells for Ne, Ar, Kr, and Xe, respectively, and compare them with the RRPDA results,⁷ as well as with experimental data.^{18–20,24–28} The RTDLDA calculation for Ne, shown in Fig. 5, is seen to be larger than the experimental measurements^{18–20} by a factor of approximately 2 throughout the interval of energies. The RRPDA, on the other hand, underestimates the partial cross section, although by a smaller factor and over a more limited range of energies. For higher energies the RRPDA is in reasonable agreement with experiment. The RPAE of Amusia and Cherepkov,¹⁰ shown here in the dashed–double-dotted curve, is in better agreement with experiment. The agreement of the RPAE results with experiment may be fortuitous, since alternative non-relativistic RPAE calculations by Chang²⁹ are in very good agreement with the RRPDA.

In the case of Ar, the partial cross section of the $3s$ shell, shown in Fig. 6, has a Cooper minimum near 1.5 a.u.; the RTDLDA is in general agreement with the measured data^{18,20,24,25} near the minimum, but again overesti-

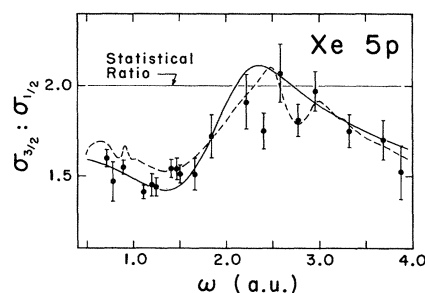


FIG. 9. Branching ratio of the $5p$ shell of Xe as a function of photon energy ω . Experiment: \bullet , Krause *et al.* (Ref. 31). Theory: —, RTDLDA, this work; ---, RRPDA, Johnson and Cheng (Ref. 7).

mates the cross section near the subsequent maximum. The RRPA is found to be in better agreement with the somewhat indecisive experimental data.

We have not illustrated the Kr $4s$ cross section calculated in the RTDLDA because of the lack of experimental measurements: only one data point has been published in the literature.²⁶ It will therefore suffice to mention that the RTDLDA and RRPA calculations of σ_{4s} for Kr exhibit the same behavior as for Ar and Xe. The RTDLDA provides an excellent description of the Xe $5s$ cross section in the region of the minimum, as shown in Fig. 7, although again it overestimates experimental values²⁶⁻²⁸ at higher energies.

IV. BRANCHING RATIOS OF THE np SUBSHELLS

The ratio of the partial cross sections of the $np_{3/2}$ and $np_{1/2}$ components of the np shell, the branching ratio, provides an interesting and detailed test of photoionization theories, since nonrelativistically this ratio has the energy-independent value of 2, and therefore any structure seen in the branching ratio is due to relativistic (mainly spin-orbit) effects.

The RTDLDA branching ratio for the $2p$ shell of Ne is, to within a few percent, uniformly equal to the nonrelativistic ratio of 2, as one expects for a light atom where relativistic effects are very small. The RTDLDA branching ratios for the Ar $3p$ and Kr $4p$ subshells, shown in Fig. 8, and the corresponding RRPA results, are notably different from the constant value of 2. Although both theories give somewhat different results for lower energies, the general trends and shapes of the corresponding curves are similar, except in the vicinity of the thresholds. The RRPA results agree better with the measured values near the thresholds,³⁰ 1.93 for Ar and 1.77 for Kr, than the results of the RTDLDA.

The theoretical branching ratios for the Xe $5p$ subshell are compared with recent experimental data³¹ in Fig. 9. A feature which is apparent in Fig. 9 is that autoionizing resonance structure is absent in the RTDLDA curve. The RRPA curve, on the other hand, exhibits some of the experimentally observed resonance structure in the vicinity of the thresholds of the $4d_{3/2}$ and $4d_{1/2}$ subshells. The absence of resonances in the RTDLDA is due to the physically incorrect behavior of the exchange-correlation potential at large distances.²² The one-electron potential in the RTDLDA becomes neutral asymptotically, while in the RRPA it approaches the ionic Coulomb potential.

V. PHOTOELECTRON ANGULAR-DISTRIBUTION ASYMMETRY PARAMETERS FOR np SUBSHELLS

The values of the angular-distribution asymmetry parameters $\beta_{np_{1/2}}$ and $\beta_{np_{3/2}}$ of the two np subshells of Ne and Ar are very close to one another due to small relativistic effects. Therefore, only the weighted-average asymmetry parameter

$$\beta_{np} = \frac{\sigma_{np_{1/2}}\beta_{np_{1/2}} + \sigma_{np_{3/2}}\beta_{np_{3/2}}}{\sigma_{np_{1/2}} + \sigma_{np_{3/2}}}$$

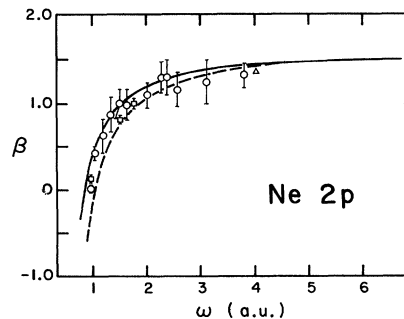


FIG. 10. Averaged angular-distribution asymmetry parameter of the $2p$ shell of Ne as a function of photon energy ω . Experiment: \circ , Codling *et al.* (Ref. 33); \square , Dehmer *et al.* (Ref. 32); \triangle , Wuilleumier and Krause (Ref. 34). Theory: —, RTDLDA, this work; ---, RRPA, Johnson and Cheng (Ref. 7).

is plotted for Ne in Fig. 10 and for Ar in Fig. 11. The theoretical curves are compared with the measured values (Ne, Refs. 32-34; Ar, Refs. 32 and 35) in the same figures. Both the RRPA and RTDLDA give results for Ne and Ar in good agreement with measurements.

Since relativistic effects are noticeable for Kr and Xe, the RTDLDA results and the RRPA results are plotted for individual $np_{3/2}$ and $np_{1/2}$ subshells in Fig. 12 for Kr and in Fig. 13 for Xe, where they are compared with measured data (Kr, Refs. 32, 36, and 37; Xe, Ref. 31). Both the RTDLDA and RRPA results are again in good agreement with the experimental measurements for Kr and Xe.

VI. PHOTOELECTRON ANGULAR-DISTRIBUTION ASYMMETRY PARAMETER FOR ns SUBSHELLS

It is interesting to observe the development of relativistic effects in the asymmetry parameter for the ns shell of a rare-gas atom. Relativistically, β_{ns} departs from the predicted nonrelativistic constant value of 2 whenever the amplitude of the excited triplet state, which vanishes in the nonrelativistic case, is not small compared with the amplitude of the excited singlet state.⁷ This generally

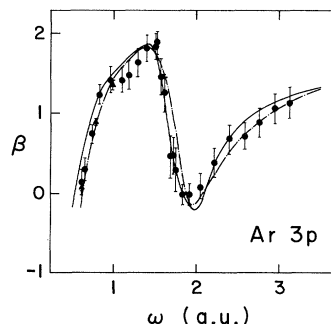


FIG. 11. Averaged angular-distribution asymmetry parameter of the $3p$ shell of Ar as a function of photon energy ω . Experiment: \circ , Houlgate *et al.* (Ref. 35); \square , Dehmer *et al.* (Ref. 32). Theory: —, RTDLDA, this work; ---, RRPA, Johnson and Cheng (Ref. 7).

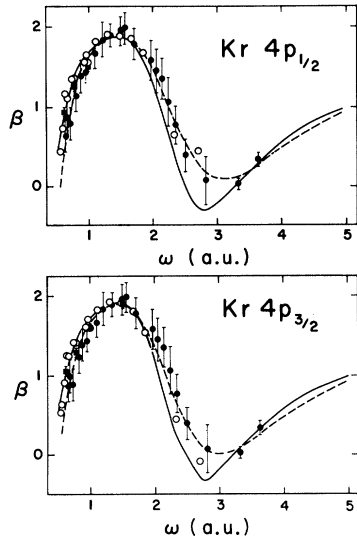


FIG. 12. Angular-distribution asymmetry parameter of the $4p_{1/2}$ (upper panel) and $4p_{3/2}$ (lower panel) subshells of Kr as a function of photon energy ω . Experiment: \circ , Krause *et al.* (Ref. 36); \blacklozenge , Miller *et al.* (Ref. 37); \blacktriangle , Dehmer *et al.* (Ref. 32). Theory: —, RTDLDA, this work; - - -, RRP, Johnson and Cheng (Ref. 7).

occurs near the Cooper minimum, where the singlet amplitude is small.

Values of the asymmetry parameter β_{ns} for Ne predicted by both the RRP and RTDLDA are found to be very close to 2, since there is no $2s$ Cooper minimum for Ne. For the other atoms considered, β_{ns} drops below 2 near the Cooper minimum. The minima in the curves for β_{ns} in the RTDLDA are found to be shallower than those predicted by the RRP. For example, the minimum in β_{ns} for Ar calculated in the RTDLDA ($\beta_{3s,\min}^{\text{RTDLDA}} = 1.99$) is extremely shallow compared to the corresponding

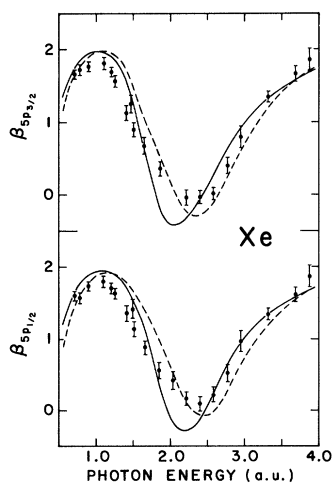


FIG. 13. Angular-distribution asymmetry parameter of the $5p_{1/2}$ (upper panel) and $5p_{3/2}$ (lower panel) subshells of Xe as a function of photon energy ω . Experiment: \blacklozenge , Krause *et al.* (Ref. 31). Theory: —, RTDLDA, this work; - - -, RRP, Johnson and Cheng (Ref. 7).

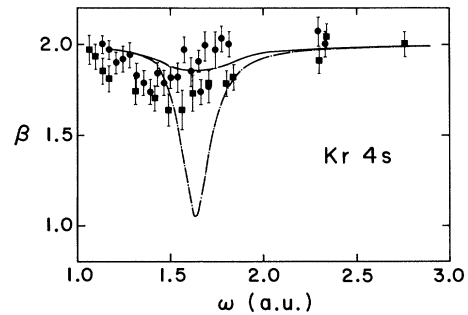


FIG. 14. Angular-distribution asymmetry parameter of the $4s$ shell of Kr as a function of photon energy ω . Experiment: \blacklozenge , Fahlman *et al.* (Ref. 38); \blacktriangle , Derenbach and Schmidt (Ref. 39). Theory: —, RTDLDA, this work; - - -, RRP, Johnson and Cheng (Ref. 7).

minimum found in the RRP ($\beta_{3s,\min}^{\text{RRP}} = 1.6$).⁷

Comparison of the theoretical results for Kr shown in Fig. 14, with the very recent measurements of Fahlman *et al.*³⁸ and Derenbach and Schmidt³⁹ favors the present RTDLDA calculations over the RRP, although there is still appreciable disagreement.

The comparison between the RTDLDA and recent precision measurements^{28,40} is even more favorable in the case of xenon, as shown in Fig. 15. The RTDLDA results are in good agreement with experimental data,^{28,40-42} whereas the RRP, although predicting the general behavior seen experimentally, overestimates the depth of the minimum in β_{ns} .

There are some physical effects, not accounted for by the RRP, which may explain the discrepancy of the RRP with the experimental data for the asymmetry parameter β_{ns} of Kr and Xe around the Cooper minimum. As suggested by Wendin and Starace in their analysis of Xe $5s$ photoionization,⁴³ interactions between photoioni-

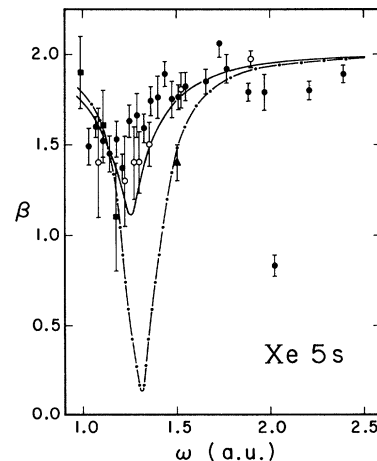


FIG. 15. Angular-distribution asymmetry parameter of the $5s$ shell of Xe as a function of photon energy ω . Experiment: \blacklozenge , Dehmer and Dill (Ref. 40); \blacklozenge , Fahlman *et al.* (Ref. 29); \blacklozenge , Derenbach and Schmidt (Ref. 41); \blacklozenge , White *et al.* (Ref. 42). Theory: —, RTDLDA, this work; - - -, RRP, Johnson and Cheng (Ref. 7).

zation main lines and satellites could be a possible reason for this discrepancy, since this interaction is usually very small, but may have measurable effects when the dominant photoionization transition amplitude is small. The RTDLDA includes such interactions in an average way. Another possible explanation for the discrepancy between theory and experiment is the neglect of the electric quadrupole contribution to the transition amplitude as discussed by Wang *et al.*⁴⁴ They have found that in photoionization of the 5s shell of Sn, interference of dipole and quadrupole transition amplitudes leads to a significant correction to the pure dipole results for the differential cross section in the neighborhood of the cross-section minimum. Neither the RRPDA, nor the RTDLDA calculations performed to date include the contribution of electric quadrupole transitions.

VII. SPIN POLARIZATION OF PHOTOELECTRONS

The photoelectron spin polarization may be expressed in a rectangular coordinate system with the z axis coinciding with the direction of the photoelectron momentum \vec{p} , the y axis coinciding with the direction of the vector $(\vec{k} \times \vec{p})$, \vec{k} being the photon momentum, and the x axis coinciding with the direction of the vector $(\vec{k} \times \vec{p}) \times \vec{p}$.⁴⁵ The components of spin polarization of photoelectrons ejected by incident circularly polarized light are expressed in terms of the three spin-polarization parameters ξ , η , and ζ ,⁴⁵

$$P_x = \pm \xi \sin \theta / F(\theta),$$

$$P_y = \eta \sin \theta \cos \theta / F(\theta),$$

$$P_z = \pm \zeta \cos \theta / F(\theta),$$

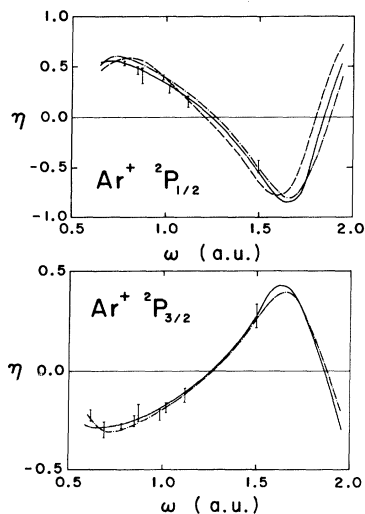


FIG. 16. Spin-polarization parameter of the $3p_{1/2}$ (upper panel) and $3p_{3/2}$ (lower panel) subshells of Ar as a function of photon energy ω . Experiment: \square , Heinzmann *et al.* (Ref. 46). Theory: —, RTDLDA, this work; - - - -, RRPDA, Huang *et al.* (Ref. 14); · · · ·, RPAE, Cherepkov (Ref. 16) with sign reversed.

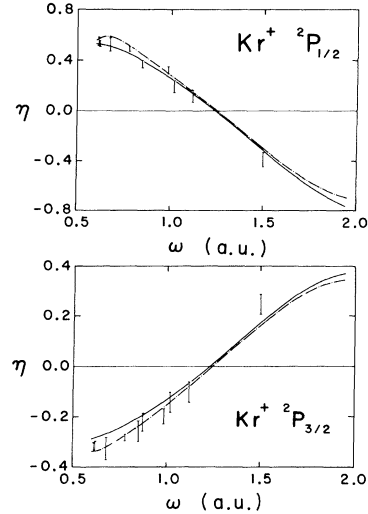


FIG. 17. Spin-polarization parameter of the $4p_{1/2}$ (upper panel) and $4p_{3/2}$ (lower panel) subshells of Kr as a function of photon energy ω . Experiment: \square , Heinzmann *et al.* (Ref. 46). Theory: —, RTDLDA, this work; - - - -, RRPDA, Huang *et al.* (Ref. 14).

with

$$F(\theta) = 1 - \frac{1}{2} \beta P_2(\cos \theta),$$

where θ is the angle between the photoelectron and photon momenta, and where the plus and minus signs indicate positive and negative helicity, respectively.

We have considered here the spin polarization of photoelectrons from Ar, Kr, and Xe by unpolarized light, in which case only the polarization component P_y is nonvanishing. In Figs. 16–18 the results of our RTDLDA calculations of the parameter η for np subshells are present-

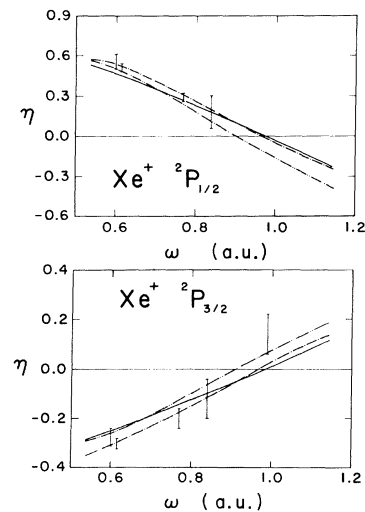


FIG. 18. Spin-polarization parameter of the $5p_{1/2}$ (upper panel) and $5p_{3/2}$ (lower panel) subshell of Xe as a function of photon energy ω . Experiment: \square , Heinzmann *et al.* (Ref. 47). Theory: —, RTDLDA, this work; - - - -, RRPDA, Huang *et al.* (Ref. 14); · · · ·, RPAE, Cherepkov (Ref. 16) with sign reversed.

ed, respectively, for Ar, Kr, and Xe, together with the RRPAs results,¹⁴ and with the experimental data (Ar and Kr, Ref. 46; Xe, Ref. 47). The theoretical results from the nonrelativistic RPAE calculations of Cherepkov¹⁶ for Ar and Xe are also presented in Figs. 16 and 18.

It is seen from the comparisons in Figs. 16–18 that the RTDLDA results agree with experimental data as well as the RRPAs. The nonrelativistic RPAE results¹⁶ for Ar and Xe are also seen to be in good agreement with both the relativistic calculations and with the experimental measurements.

VIII. COMPARISON OF EXCHANGE-CORRELATION POTENTIALS

We have mentioned in the Introduction that the photoionization parameters are not independent of the exchange-correlation potential used. To illustrate the sensitivity of the RTDLDA to the choice of the exchange-correlation potential, we show in Fig. 19 three calculations of the parameter β_{ns} for Xe using three different parametrizations of the exchange and correlation potentials. The Gunnarsson-Lundqvist potential,⁴⁸ used to calculate the dashed curve, treats exchange in the Kohn-Sham approximation and correlation semiempirically. Exchange is also treated in the Kohn-Sham approximation in the Perdew-Zunger case, which is used to obtain the solid curve in Fig. 19; however, the correlation potential, while still semiempirical, has the more elaborate parametrization, given by Perdew and Zunger, of Ceperley's data.⁴⁹ (We have *not* included the self-interaction connection suggested by Perdew and Zunger.) Finally, the Ramana-Rajagopal exchange-correlation potential, which is used to produce the dotted curve in Fig.

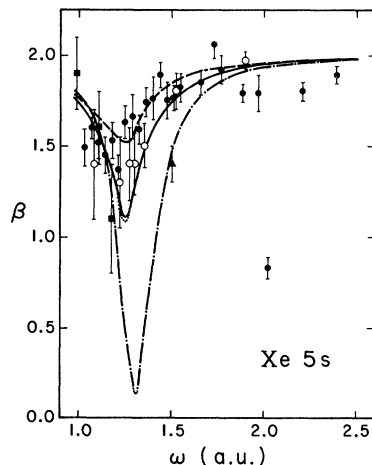


FIG. 19. Angular-distribution asymmetry parameter of the 5s shell of Xe as a function of photon energy ω . Experiment: \blacktriangle , Dehmer and Dill (Ref. 41); \blacktriangledown , White *et al.* (Ref. 42); \bullet , Fahlman *et al.* (Ref. 28); \circ , Derenbach and Schmidt (Ref. 40). Theory: —, RTDLDA with Perdew-Zunger exchange-correlation potential, this work; ---, RTDLDA with Gunnarsson-Lundqvist exchange-correlation potential, this work; \cdots , Ramana-Rajagopal exchange-correlation potential, this work; - - - - -, RRPAs, Johnson and Cheng (Ref. 7).

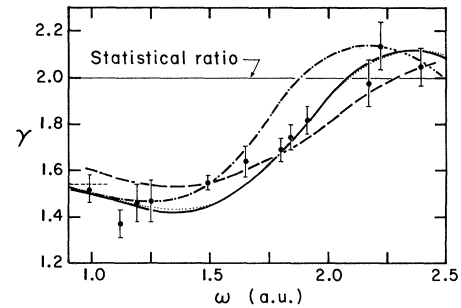


FIG. 20. Branching ratio of the 5p shell of Xe as a function of energy ω . Experiment: \blacktriangledown , Willeumier *et al.* (Ref. 52). Theory: —, RTDLDA with Perdew-Zunger exchange-correlation potential, this work; - - - - -, RTDLDA with Gunnarsson-Lundqvist exchange-correlation potential, this work; \cdots , Ramana-Rajagopal exchange-correlation potential, this work; - - - - -, RRPAs, Johnson and Cheng (Ref. 7).

19, is derived from first principles.^{12,13,50} Here the exchange includes the frequency-dependent Breit correction to the nonrelativistic Kohn-Sham approximation. The correlation potential used in the Ramana-Rajagopal case is the relativistic generalization of the ring sum correlation potential calculated by von Barth and Hedin.⁵¹ Although the oldest single measurement of β_{5s} (Ref. 41) lies on the RRPAs curve, which is shown as the dashed-dotted curve in Fig. 19, the present RTDLDA results for all three exchange-correlation potentials are closer to the more recent measurements^{28,40} of β_{5s} than the RRPAs results.

In Fig. 20 a similar comparison between the three choices for exchange-correlation potential and experiment is made for the 5p branching ratio of Xe.⁵² The Gunnarsson-Lundqvist potential leads to predictions that depart appreciably from predictions of the Perdew-Zunger and Ramana-Rajagopal models. We interpret the consistency between the predictions of the latter two choices of exchange-correlation potentials as an indication of their essential correctness: they have been determined by two very different techniques and yet yield results in excellent agreement. The remaining discrepancies between the calculations made using the Ramana-Rajagopal and Perdew-Zunger potentials may be ascribed principally to the difference in treatment of relativistic effects. Given the precision of experimental technique it is impossible to state a preference for either. We have therefore arbitrarily chosen the Perdew-Zunger parametrization.

Relativistic corrections to the exchange-correlation potential increase in importance with increasing atomic number. It is possible, therefore, that studies of photoionization for elements heavier than Xe can provide a clearer indication of which potential is most appropriate for studies of excitations of atomic systems. Such a study remains to be undertaken.

ACKNOWLEDGMENTS

The authors are grateful to M. Idrees for producing the preliminary forms of several graphs and the list of refer-

ences. We thank A. Fahlman and M. O. Krause, and H. Derenbach and V. Schmidt for communicating their results in preprint form. We are also grateful to A. Fahlman, M. O. Krause, and K.-N. Huang for numerical ver-

sions of their results. This work was supported in part by the National Science Foundation under Grant No. PHY-83-08136.

- *On leave of absence from the Boris Kidrich Institute, P.O. Box 522, 11001 Beograd, Yugoslavia.
- ¹A. Zangwill and P. Soven, *Phys. Rev. A* **21**, 1561 (1980); *Phys. Rev. Lett.* **45**, 204 (1980).
 - ²J. A. R. Samson, *Handbuch der Physik*, Vol. 31 of *Encyclopedia of Physics* (Springer, Heidelberg, 1983), pp. 123–213.
 - ³F. A. Parpia and W. R. Johnson, *J. Phys. B* **16**, L375 (1983).
 - ⁴F. A. Parpia and W. R. Johnson, *J. Phys. B* **17**, 531 (1984).
 - ⁵D. A. Liberman and A. Zangwill, *Comput. Phys. Commun.* (in press).
 - ⁶W. R. Johnson and C. D. Lin, *Phys. Rev. A* **20**, 964 (1979).
 - ⁷W. R. Johnson and K. T. Cheng, *Phys. Rev. A* **20**, 978 (1979).
 - ⁸P. L. Altick and A. E. Glasgold, *Phys. Rev.* **133**, A632 (1964).
 - ⁹A. Dalgarno and G. A. Victor, *Proc. R. Soc. London, Ser. A* **291**, 291 (1966).
 - ¹⁰M. Ya. Amusia and N. A. Cherepkov, *Case Stud. At. Phys.* **5**, 47 (1975).
 - ¹¹G. Wendin, in *Photoionization and Other Probes of Many-Electron Interactions*, edited by F. J. Wuilleumier (Plenum, New York, 1976), pp. 61–82.
 - ¹²A. K. Rajagopal, *J. Phys. C* **11**, L943 (1978).
 - ¹³A. H. MacDonald and S. H. Vosko, *J. Phys. C* **12**, 2977 (1979).
 - ¹⁴K.-N. Huang, W. R. Johnson, and K. T. Cheng, *Phys. Rev. Lett.* **43**, 1658 (1979).
 - ¹⁵K.-N. Huang, W. R. Johnson, and K. T. Cheng, *At. Data Nucl. Data Tables* **26**, 33 (1981).
 - ¹⁶N. A. Cherepkov, *J. Phys. B* **11**, L435 (1978).
 - ¹⁷J. Cooper and R. N. Zare, in *Lectures in Theoretical Physics*, edited by S. Geltman, K. T. Mahantappa, and W. E. Britten (Gordon and Breach, New York, 1969), Vol. XI-C, pp. 317–337.
 - ¹⁸J. A. R. Samson, *Adv. At. Mol. Phys.* **2**, 177 (1966).
 - ¹⁹W. S. Watson, *J. Phys. B* **5**, 2292 (1972).
 - ²⁰G. V. Marr and J. B. West, *At. Data Nucl. Data Tables* **18**, 497 (1976).
 - ²¹J. B. West and J. Morton, *At. Data Nucl. Data Tables* **22**, 103 (1978).
 - ²²A. Zangwill, in *Atomic Physics 8*, edited by I. Lindgren, A. Rosen, and S. Svanberg (Plenum, New York, 1983).
 - ²³G. Wendin, *J. Phys. B* **6**, 42 (1973).
 - ²⁴K. H. Tan and C. E. Brion, *J. Electron Spectrosc.* **13**, 77 (1978).
 - ²⁵M. Y. Adam, F. Wuilleumier, S. Krummacher, N. Sandner, V. Schmidt, and W. Mehlhorn, *J. Electron Spectrosc.* **15**, 211 (1979).
 - ²⁶J. A. R. Samson, and J. L. Gardner, *Phys. Rev. Lett.* **33**, 671 (1974).
 - ²⁷T. Gustafsson, *Chem. Phys. Lett.* **51**, 383 (1977).
 - ²⁸A. Fahlman, T. A. Carlson, and M. O. Krause, *Phys. Rev. Lett.* **50**, 1114 (1983).
 - ²⁹T. N. Chang, *Phys. Rev. A* **15**, 2392 (1977).
 - ³⁰J. A. R. Samson, J. L. Gardner, and A. F. Starace, *Phys. Rev. A* **12**, 1459 (1975).
 - ³¹M. O. Krause, T. A. Carlson, and P. R. Woodruff, *Phys. Rev. A* **24**, 1374 (1981).
 - ³²J. L. Dehmer, W. A. Chupka, J. Berkowitz, and W. T. Jivery, *Phys. Rev. A* **12**, 1966 (1975).
 - ³³K. Codling, R. G. Houlgate, J. B. West, and P. R. Woodruff, *J. Phys. B* **9**, L83 (1976).
 - ³⁴F. Wuilleumier and M. O. Krause, *Phys. Rev. A* **10**, 242 (1974).
 - ³⁵R. G. Houlgate, J. B. West, K. Codling, and G. V. Marr, *J. Electron Spectrosc.* **9**, 205 (1976).
 - ³⁶M. O. Krause (private communication).
 - ³⁷D. L. Miller, J. D. Dow, R. G. Houlgate, G. V. Marr, and J. B. West, *J. Phys. B* **10**, 3205 (1977).
 - ³⁸A. Fahlman, T. A. Carlson, and M. O. Krause (private communication and unpublished).
 - ³⁹H. Derenbach and V. Schmidt, *J. Phys. B* **17**, 83 (1984).
 - ⁴⁰H. Derenbach and V. Schmidt, *J. Phys. B* **16**, L337 (1983).
 - ⁴¹J. L. Dehmer and D. Dill, *Phys. Rev. Lett.* **37**, 1049 (1976).
 - ⁴²M. G. White, S. H. Southworth, P. Kobrin, E. D. Poliakoff, R. A. Rosenberg, and D. A. Shirley, *Phys. Rev. Lett.* **43**, 1661 (1979).
 - ⁴³G. Wendin and A. F. Starace, *Phys. Rev. A* **28**, 3143 (1983).
 - ⁴⁴M. S. Wang, Y. S. Kim, R. A. Pratt, and A. Ron, *Phys. Rev. A* **25**, 857 (1982).
 - ⁴⁵K.-N. Huang, *Phys. Rev. A* **22**, 223 (1980).
 - ⁴⁶U. Heinzmann, G. Schonhense, and J. Kessler, *J. Phys. B* **13**, L153 (1980).
 - ⁴⁷U. Heinzmann, G. Schonhense, and J. Kessler, *Phys. Rev. Lett.* **42**, 1603 (1979).
 - ⁴⁸O. Gunnarsson and B. I. Lundqvist, *Phys. Rev. B* **13**, 4274 (1976).
 - ⁴⁹D. M. Ceperley, *Phys. Rev. B* **18**, 3126 (1978); J. P. Perdew and A. Zunger, *ibid.* **23**, 5048 (1981).
 - ⁵⁰M. V. Ramana and A. K. Rajagopal, *Phys. Rev. A* **24**, 1689 (1981).
 - ⁵¹U. von Barth and L. Hedin, *J. Phys. C* **5**, 1629 (1972).
 - ⁵²F. Wuilleumier, M. Y. Adam, P. Dhez, N. Sandner, V. Schmidt, and W. Mehlhorn, *Phys. Rev. A* **16**, 646 (1977).